15th Australasian Fluid Mechanics Conference
The University of Sydney, Sydney, Australia
13-17 December 2004

# The Effect of Density Ratio on the Mean Spread Rate of a Low Pressure Drop Oscillating Jet Nozzle

**G. England, P.A.M. Kalt, G.J. Nathan and R.M. Kelso**

School of Mechanical Engineering
The University of Adelaide, SA, 5005 AUSTRALIA

## Abstract

Particle Image Velocimetry measurements were obtained in the highly unsteady turbulent flow issuing from a triangular oscillating jet (TOJ) nozzle into a fluid of different density. The TOJ nozzle comprises a triangular jet partially confined within an axi-symmetric chamber that produces a large-scale flow oscillation which is analogous to that in a precessing jet nozzle previously investigated. The initial spreading angle of the emerging jet was found to depend upon the density ratio, but in a more complex and different way to that of an unconfined jet. Instead, an increase in the density ratio of the jet fluid to the surroundings is found to be analogous to a decrease in the ratio of the nozzle length to diameter.

## Introduction

Fluidic precessing jet (FPJ) flames of natural gas have high radiant heat transfer, high burn-out and low emissions of oxides of nitrogen ($NO_x$) and are therefore attractive in industrial applications such as cement and lime production. In such applications, FPJ flames have been demonstrated to reduce $NO_x$ emissions by between 40-70% [10] while achieving a fuel saving of up to 5% for an equivalent product output. Additionally, the product quality is improved due to the shift in heat transfer profile toward the front of the kiln [6]. More recently they have been applied to pulverised fuels, with promising results [8,12].

The FPJ flow has been studied extensively at the University of Adelaide because of its scientific interest and immediate relevance to industrial applications. However the flow is highly unsteady and complex, making its characterisation and optimisation difficult. The unsteadiness allows more rapid initial spread and decay than is possible for a steady jet, and is deduced to be the primary cause of the benefits [9]. However, the large expansion ratio within the nozzle results in a large pressure drop across the burner. While this is not an obstacle when firing natural gas, which is usually available at high pressure, it is a significant barrier in pulverised fuel applications where air must be pressurised on-site.

A new burner, known as the triangular oscillating jet (TOJ) nozzle, has been developed to provide an oscillating flow which is closely related to that of the FPJ nozzle but with a lower pressure drop. The TOJ nozzle has been shown to produce large-scale oscillations, large initial spreading and rapid near-field velocity decay rate of similar trend, but reduced magnitude, to those observed from the FPJ nozzle [4]. However, the temperature of the co-flowing (secondary) combustion air in a rotary kiln is high – typically 600-1200°C, and this temperature varies both during operation and from site to site. The high temperature leads to a density difference between the jet fluid and the co-flow fluid. The influence of this density difference on the internal or emerging flows has not been investigated previously. The present study seeks to address this by measurement of the near-field jet spreading from the TOJ nozzle using a range of jet fluids of different density.

## Experimental Method

Velocity measurements were performed using a digital cross-correlation particle image velocimetry (DPIV) system at the Turbulence Energy and Combustion Laboratory of the University of Adelaide.

## Experimental Setup

The TOJ nozzle is similar to that described by Lee *et al.* [4]. It utilises a triangular orifice partially confined by an axisymmetric chamber with a small lip at the nozzle exit (Figure 1). The chamber diameter, $D$, is 26.5 mm and the exit lip diameter, $d_2$, is 21.8 mm. The triangular orifice is equilateral, its size described by the diameter of a circular orifice with equivalent cross-sectional area, $d_{eq}$. In this study, non-reacting TOJ flows with an expansion ratio, $D/d_{eq}$, of 3.5 are examined.

The length of the nozzle, L, is, for most of the work, selected to satisfy the ratio $L$/D = 2.49. This is based on the work of Lee *et al*. [4], who determined this to be the optimum length to diameter ratio for maximum spread when the density ratio $\rho_j/\rho_a$ = 1. However for the case with carbon dioxide as the working fluid, $L/D$ ratios of 2.11, 2.30 and 2.68 are also examined.

The working fluids, carbon dioxide, argon, air and a helium-air mixture, were introduced through the nozzle into ambient air. This gives density ratios, $\rho_j/\rho_a$, of 1.56, 1.39, 1 and 0.57 respectively. The jet Reynolds number, calculated using the effective orifice diameter; $\mathrm{Re} = \rho\, d_{eq} u/\mu$ = 60,000. Both the jet, and an ambient air co-flow of negligible momentum, were seeded with atomised olive oil with a nominal droplet diameter of 0.6μm. These droplets are effective flow tracers even in the high shear regions at the edge of the jet.

The laser sheet was aligned with the nozzle centreline and configured to provide sufficiently uniform intensity through the exit plane. The orientation of the triangular orifice with respect to the light sheet is shown in Figure 1. The camera was positioned to capture the emerging flow over the range $0 < x/D \leq 4$.

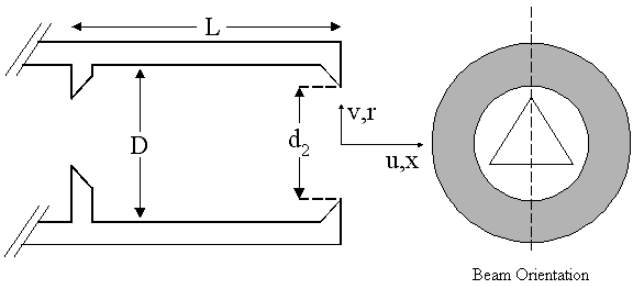


Figure 1. Notation for the Triangular Oscillating Jet (TOJ) nozzle and the laser beam orientation.

## Lasers and Optics

The particles are illuminated by the second harmonic (λ = 532 nm) of a Quantel Brilliant Twins double-cavity pulsed Nd:YAG laser. The output energy of each pulse is ~250 mJ. The laser beams are directed towards the imaged area using 2 dichroic mirrors, and are formed into a laser sheet approximately 1.9 mm

thick in the imaged area using a series of cylindrical lenses. This thickness of the laser sheet is necessary to avoid significant loss of image pairs due to the large out-of-plane motion in these unsteady flows. The light sheet thickness thus becomes a limiting dimension in the spatial resolution of the measurement.

A Kodak MegaPlus ES1.0 PIV camera, operated in the triggered double exposure mode, was used to record the Mie-scattered particle images. The images were collected through a Nikon ED 70-300 telephoto lens. The dimensions of the CCD array are 1008 pixels by 1018 pixels. The imaged region was 100 mm by 101 mm, with each pixel corresponding to a region measuring 100 µm by 101 µm. The time delay between laser pulses was set to 20 µs, which was optimised for a PIV interrogation window of 32 × 32 pixels, with a 50% overlap. This results in an effective resolution for the velocity measurements of 3.2 mm, which is comparable with the light sheet thickness. The resulting vector field contains 62 by 62 vectors.

## Timing

A Hamag signal generator producing 10 Hz TTL output initiated the timing of data collection. This 10 Hz output was used to trigger a Stanford Research Systems DG-535 delay generator which, in turn, triggered both the laser flash-lamps and the camera. The delay between the laser flash-lamp and the Q-Switch was set by internal timing electronics, so that the delay between laser pulses could be altered without adjusting the Q-switch delay or the laser energy. Data were transferred from the camera at 20 Hz into a memory buffer on the data storage computer. After each run, the entire dataset of PIV image pairs was saved to hard disk for subsequent processing. The size of the data set was limited by the buffer size to 360 image pairs.

## PIV Processing

Processing of the PIV image pairs was performed using Pivtec's PivView (v 1.7.5) software. A 2-pass Hart correlation algorithm was used to correlate between the image pairs. The correlation image was scanned for peaks using a centroid-hunting algorithm on a roaming 3 × 3 pixel mask. This method gives sub-pixel accuracy.

Outliers (erroneous vectors) are detected by comparison with the neighbourhood average. Where possible, outliers are replaced by a suitable, alternative peak from the correlation plane but are otherwise deleted. The total proportion of deleted vectors is less than 2% in the worst case.

## RESULTS

Data analysis is carried out for the axial component, $u$ of the time averaged velocity field. Normalisation is typically applied relative to the bulk mean orifice velocity $u_{or}$. Figure 2 shows the time averaged flow field, $u/u_{or}$, for the TOJ with $L/D$ = 2.49 and $\rho_j/\rho_a$ = 1.56. This is typical of the time averaged flow field in all cases. Half widths are used to asses the spreading angle of the emerging TOJ jet. Half widths are obtained from the time averaged flow field. The mean spread, $r_{1/2}$, is taken to be the average of that on either side of the nozzle axis noting the asymmetry resulting from the triangular orifice [4]. The orientation of the light is such that the left side of the image is aligned with an apex of the orifice.

## Effect of $\rho_j/\rho_a$

Figure 3 shows the mean half widths, $r_{1/2}$, for the TOJ nozzle at each of the density ratios, $\rho_j/\rho_a$, investigated. This figure shows that the greatest spread rate of the jet emerging from the nozzle is achieved when the density ratio, $\rho_j/\rho_a$, is 1. At first sight, this appears to contradict the well known dependence of the spreading angle for a free jet, which decreases with an increase in the density ratio, as determined by Era and Saima [2] and Richards and Pitts [11].

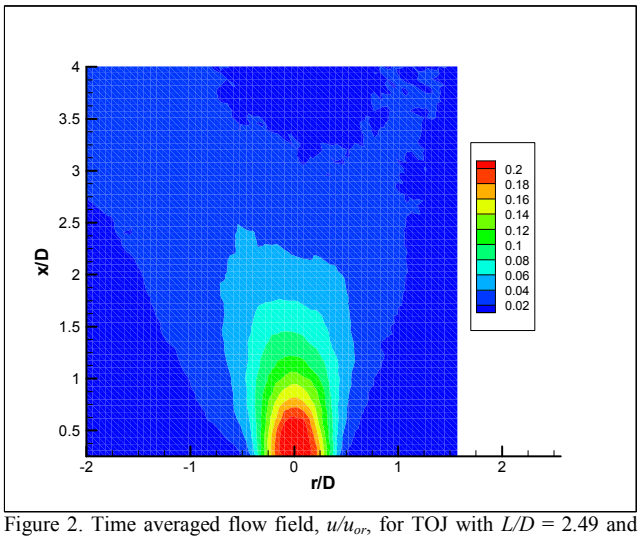


Figure 2. Time averaged flow field, $u/u_{or}$, for TOJ with $L/D$ = 2.49 and $\rho_j/\rho_a$ = 1.56.

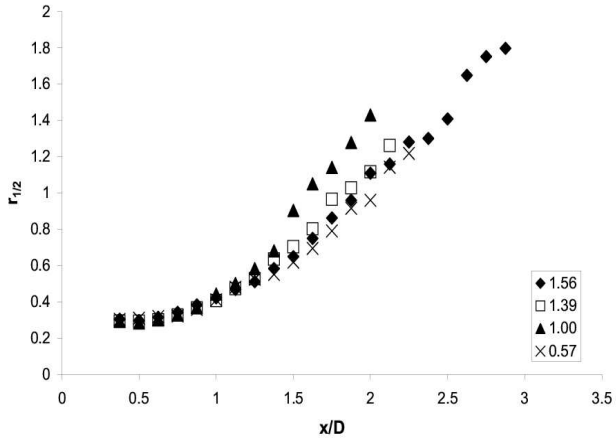


Figure 3. Mean half widths for TOJ at various $\rho_j/\rho_a$ as determined from the mean flow field.

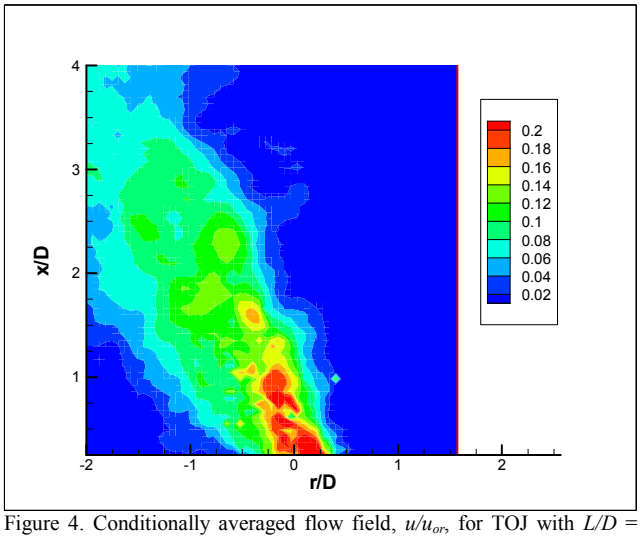


Figure 4. Conditionally averaged flow field, $u/u_{or}$, for TOJ with $L/D$ = 2.49 and $\rho_j/\rho_a$ = 1.56.

Deflection angles of the instantaneous emerging jet were determined by conditionally averaging the data. Since the angle of the jet within the plane of the light sheet depends upon its phase, those images with the greatest angles are taken to be within the plane of the light sheet. On this basis, a representative, although not absolute, measure of the instantaneous angle is taken as the average of the five image pairs with the greatest angle of deflection toward the left. These were selected by determining the slope of the linear line of best fit for maximum axial velocity for each image pair. Figure 4 shows the conditionally averaged flow field, $u/u_{or}$, for the TOJ with $L/D$ = 2.49 and $\rho_j/\rho_a$ = 1.56. This is typical of a conditionally averaged flow field. Once the conditionally averaging was complete, the spread angle was determined from the slope of the linear line of best fit for maximum axial velocity. Figure 5 shows the spread angle of the TOJ as a function of the density ratio, $\rho_j/\rho_a$. The result shown is consistent with the trend shown in figure 3.

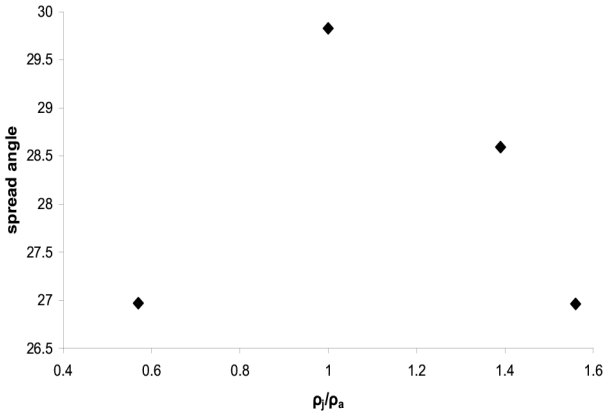


Figure 5. Deflection angle of the instantaneous emerging jet as a function of density ratio, $\rho_j/\rho_a$.

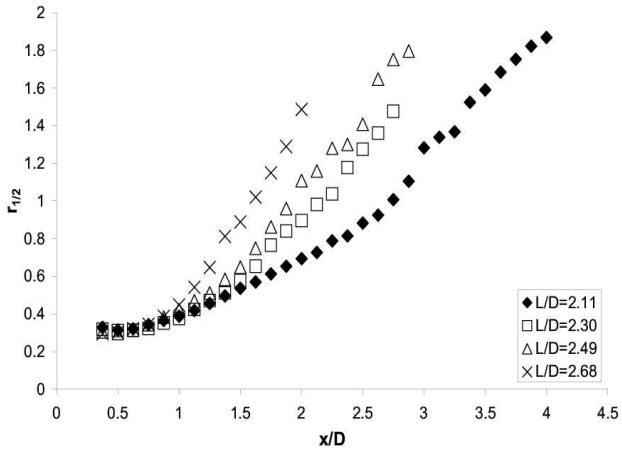


Figure 6. Mean half widths for TOJ at various $L/D$ ($\rho_j/\rho_a$ = 1.56), as determined from the time-averaged flow field.

## Effect of *L/D*

Figure 6 shows the mean half widths, $r_{1/2}$, for the TOJ nozzle at $L/D$ = 2.11, 2.30, 2.49 and 2.68 when the working fluid is carbon dioxide ($\rho_j/\rho_a$ = 1.56). This shows that increasing $L/D$ results in an increased rate of spread. This is consistent with Lee *et al.* [4] for $L/D$ less than the optimum for maximum spread. However Lee *et al.* [4] showed that when $\rho_j/\rho_a$ = 1 this optimum $L/D$ is 2.49. Figure 4 clearly shows that this is not the case when $\rho_j/\rho_a$ = 1.56 since greater spread is achieved for $L/D$ = 2.68 than $L/D$ = 2.49. This also shows that the density ratio has an effect on the spread of the jet emerging from the TOJ nozzle.

## Discussion

The apparent discrepancy between the effect of density ratio on spreading angle can be explained by consideration of the complex flow within the chamber. Lee *et al.* [4] have investigated the effect of varying the length to diameter ratio of the TOJ using air as the working fluid ($\rho_j/\rho_a$ = 1). They found that as $L/D$ was increased from zero the spread rate of the jet initially increases also. Eventually a maximum rate of spread is reached at some $L/D$, which is then defined as the optimum $L/D$. Further increasing $L/D$ leads to a decrease in the rate of jet spread. A simplified representation of this is shown in figure 7. Also shown in figure 7 is the spread inside the chamber.

Wong [13] shows that just beyond the exit plane of a FPJ nozzle the emerging jet is "kidney" shaped (although it evolves toward a circular cross-section further downstream). The lateral spreading of a jet upon reattachment to a wall is well known and can explain the evolution of a "kidney shape" within the chamber [3]. Clearly the longer the chamber, the greater this interaction with the chamber wall will be. A similar trend can be expected to occur for the TOJ nozzle. Therefore as $L/D$ is increased the spread of the jet inside the chamber is also increased, resulting in the jet both filling more of the exit plane and increasing it's interaction with the chamber walls and the exit lip (Figure 7). This implies that the spreading angle of the external jet depends upon the extent to which the emerging jet fills the exit plane of nozzle and by the interaction of the emerging jet with the exit lip.

By analogy then, it can be expected that the spreading angle of the emerging jet will also depend upon the rate of spread of the jet within the nozzle chamber, and hence on the internal density ratio. Now figure 3 shows that for the TOJ with $L/D$ = 2.49 the greatest external spread rate is achieved when the density ratio, $\rho_j/\rho_a$, is 1. This result simply reflects the fact that these dimensions were optimised for a density ratio of unity, while the flow is dependent upon the density ratio.

Nathan [7] observed that surrounding fluid is continually drawn into the FPJ chamber and entrained into the main jet. A similar phenomenon was observed for the TOJ nozzle by Lee *et al*. [5]. This induced reverse flow allows a density gradient to occur inside the nozzle chamber. It follows that when the density ratio, $\rho_j/\rho_a$, inside the chamber is lowest the internal spread will be the greatest [2,11], and will therefore result in the emerging jet filling more of the nozzle exit plane and interacting more with the chamber walls and exit lip. Hence increasing the density ratio, $\rho_j/\rho_a$, has the same effect on the external spread rate as decreasing the chamber length to diameter ratio, $L/D$.

Density gradients between the jet and surroundings rapidly decrease with downstream distance due to entrainment [1,11]. Therefore any gradient existing between the jet and the surroundings as the jet exits the nozzle will be decreased in magnitude from the initial gradient due to entrainment within the nozzle chamber. Any density gradient external of the nozzle will still have an effect on the rate of jet spread. However it is likely that this will be secondary to the interaction that take place inside the nozzle chamber where the jet shear layer is the thinnest and the density gradients are likely to be the largest.

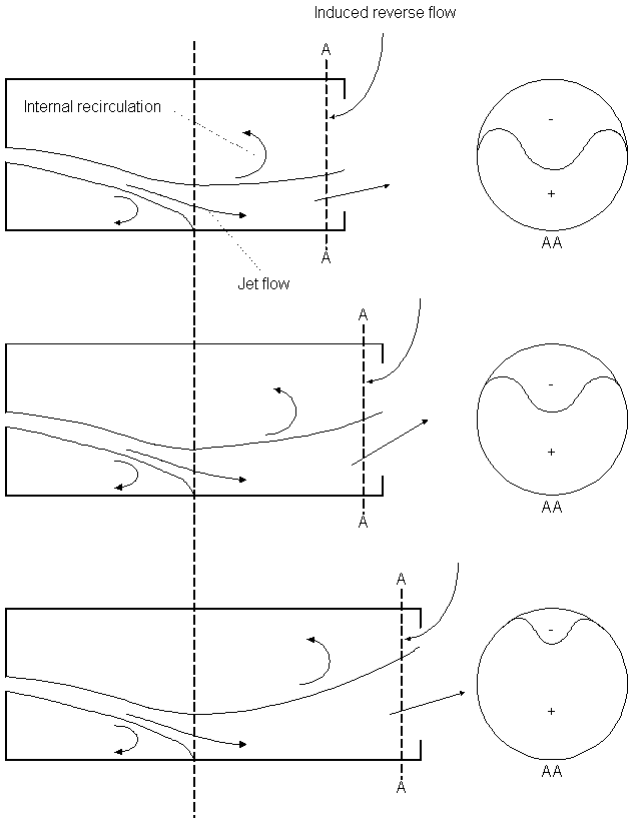


Figure 7. A simplified diagram showing the trends of the effect of varying *L/D* on the flow field within the TOJ chamber and the exit angle.

## Conclusion

The measurements of jet half widths show that, for the triangular oscillating jet nozzle whose dimensions are optimised for a unity density ratio [4], i.e. with $L/D$ = 2.49, the maximum spread occurs with this same density ratio. That is, variation of the density ratio, $\rho_j/\rho_a$, to values above or below one led to a decrease in the rate of spread.

By reference to the flow patterns within the chamber it was deduced that the effect of increasing the density ratio, $\rho_j/\rho_a$, on the spread rate is broadly analogous to the effect of decreasing the chamber length to diameter ratio, *L/D*.

Further work is required to determine the optimum *L/D* for maximum spread as a function of density ratio. More detailed investigations of the flow inside the nozzle chamber are also required to verify and quantify the proposed explanations.

## Acknowledgments

The work has been undertaken with the joint support of the Australian Research Council and FCT-Combustion through the SPIRT scheme.

## References

[1] Brown, G.L. and Roshko, A., On density effects and large structure in turbulent mixing layers, *J. Fluid Mech.,* **64(4)**, 1974, 775-816.

[2] Era, Y. and Saima, A., Turbulent mixing of gases with different densities, *B. JSME*, **20(139)**, 1977, 63-70.

[3] Law, A.W.K. and Herlina., An Experimental Study on Turbulent Circular Wall Jets, *J. Hydraul Eng.*, **128(2)**, 2002, 161-174.

[4] Lee, S.K., Lanspeary, P.V., Nathan, G.J., Kelso, R.M. and Mi, J., Low kinetic-energy loss oscillating-triangular-jet nozzles, *Exp. Therm Fluid Sci.*, **27**, 2003, 553-561.

[5] Lee, S.K., Lanspeary, P.V., Nathan, G.J. and Kelso, R.M., Surface-Flow Patterns in Oscillating-Triangular-Jet Nozzles, *15th Australasian Fluid Mechanics Conference,* Sydney, Australia, December, 2004, 13-17.

[6] Manias, C.G., and Nathan, G.J., The Precessing Jet Gas Burner – a low $NO_x$ burner providing efficiency and product quality improvements, *World Cement,* March, 1993, 4-11.

[7] Nathan, G.J., The enhanced mixing burner, PhD thesis, Department of Mechanical Engineering, University of Adelaide, Australia, 1988.

[8] Nathan, G.J., and Hill, S.J., Full Scale Assesment of the Influence of a Precessing Jet of Air on the Performance of Pulverised Coal Flame in a cement Kiln, *FCT Internal Report,* 2002.

[9] Newbold, G.J.R., Mixing and Combustion in Precessing Jet Flows, PhD Thesis, Department of Mechanical Engineering, University of Adelaide, Australia, 1998.

[10] Parham, J. J., Nathan, G. J. and Alwahabi, Z. T., Quantification of Mixing Characteristics for the Optimisation of Combustion in Rotary Kilns, *14th Australasian Fluid Mechanics Conference,* Adelaide, Australia, December, 2001, 10-14.

[11] Richards, C.D. and Pitts, W.M., Global density effects on the self-preservation behaviour of turbulent free jets, *J. Fluid Mech.*, **254**, 1993, 417-435.

[12] Smith, N.L., Megalos, N.P., Nathan, G.J., Zhang, D.K., and Smart, J. P., Precessing Jet Burners for Stable and Low NOx Pulverised Fuel Flames - Preliminary results from small-scale trials, *Fuel,* **77**, 1998, 1013-1016.

[13] Wong, C.Y., The flow within and in the near external field of a fluidic precessing jet nozzle, PhD thesis, Department of Mechanical Engineering, University of Adelaide, Australia, 2004.